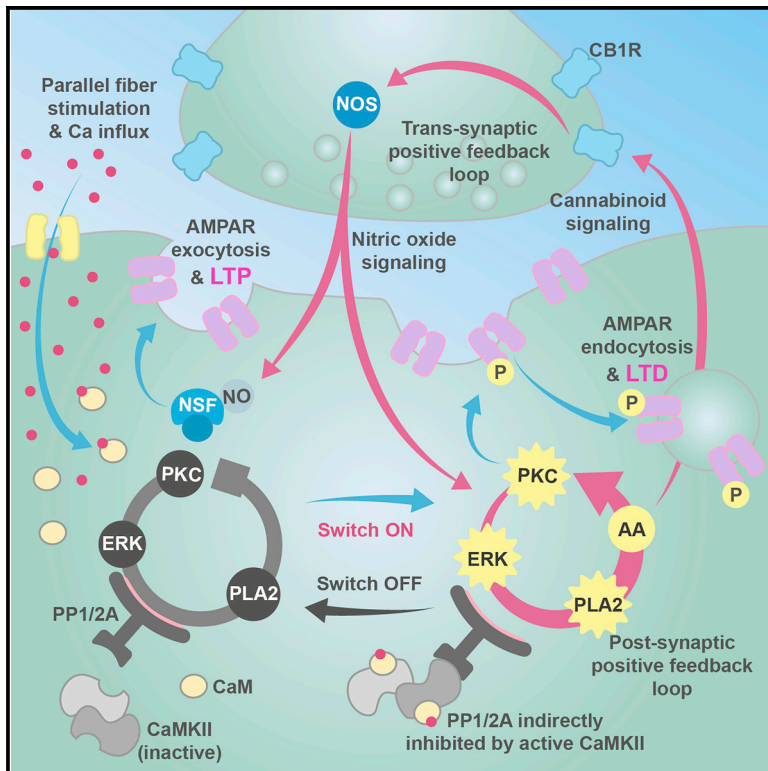


Cell Reports

Switching On Depression and Potentiation in the Cerebellum

Graphical Abstract



Authors

Andrew R. Gallimore, Taegon Kim,
Keiko Tanaka-Yamamoto,
Erik De Schutter

Correspondence

andrew.gallimore@oist.jp (A.R.G.),
erik@oist.jp (E.D.S.)

In Brief

Gallimore et al. use a bidirectional model of parallel fiber-Purkinje cell long-term depression (LTD) and long-term potentiation (LTP) to delineate the *trans*-synaptic signaling pathways that control cerebellar plasticity. An ultrasensitive on/off switch demarcates the early phase of LTD, and a *trans*-synaptic feedback loop regulates nitric oxide production during LTD and LTP.

Highlights

- Unified bidirectional model of cerebellar parallel fiber-Purkinje cell LTD and LTP
- An ultrasensitive on/off switch mechanism demarcates the early phase of LTD
- A *trans*-synaptic feedback loop regulates nitric oxide production during LTD and LTP
- LTP's frequency dependence determined by stimulus-dependent nitric oxide secretion



Switching On Depression and Potentiation in the Cerebellum

Andrew R. Gallimore,^{1,3,*} Taegon Kim,² Keiko Tanaka-Yamamoto,² and Erik De Schutter^{1,*}

¹Computational Neuroscience Unit, Okinawa Institute of Science and Technology Graduate University, Onna-son, Okinawa 904-0495, Japan

²Center for Functional Connectomics, Korea Institute of Science and Technology (KIST), Seoul 136-791, Republic of Korea

³Lead Contact

*Correspondence: andrew.gallimore@oist.jp (A.R.G.), erik@oist.jp (E.D.S.)

<https://doi.org/10.1016/j.celrep.2017.12.084>

SUMMARY

Long-term depression (LTD) and long-term potentiation (LTP) in the cerebellum are important for motor learning. However, the signaling mechanisms controlling whether LTD or LTP is induced in response to synaptic stimulation remain obscure. Using a unified model of LTD and LTP at the cerebellar parallel fiber-Purkinje cell (PF-PC) synapse, we delineate the coordinated pre- and postsynaptic signaling that determines the direction of plasticity. We show that LTP is the default response to PF stimulation above a well-defined frequency threshold. However, if the calcium signal surpasses the threshold for CaMKII activation, then an ultrasensitive “on switch” activates an extracellular signal-regulated kinase (ERK)-based positive feedback loop that triggers LTD instead. This postsynaptic feedback loop is sustained by another, *trans*-synaptic, feedback loop that maintains nitric oxide production throughout LTD induction. When full depression is achieved, an automatic “off switch” inactivates the feedback loops, returning the network to its basal state and demarcating the end of the early phase of LTD.

INTRODUCTION

The functional plasticity of neuronal synapses is indispensable for learning and the encoding of memories (Nabavi et al., 2014). Long-term depression (LTD) and long-term potentiation (LTP) at the parallel fiber-Purkinje cell (PF-PC) synapse in the cerebellum are believed to play an important role in motor learning (Ito, 2001; Yamaguchi et al., 2016; Kakegawa and Yuzaki, 2005; Malinow and Malenka, 2002; Sheng and Lee, 2001). Cerebellar plasticity is under climbing fiber (CF) control, with a calcium threshold mirroring that of the hippocampus, determining whether LTP or LTD is expressed (Coessmans et al., 2004; Malinow and Malenka, 2002). PF-PC LTD requires a local calcium concentration above this threshold, mediated by concurrent PF and CF activity at the PC, leading to protein kinase (PKC)-mediated phosphorylation and endocytosis of amino-3-hydroxy-5-methylisoxazole-4-propionic acid receptors (AMPA) (Wang and Linden, 2000; Chung et al., 2003). Postsynaptic LTP requires a lower calcium concentration and is induced

by PF stimulation alone at 1 Hz for at least 5 min (Lev-Ram et al., 2002) and can fully reverse LTD (Lev-Ram et al., 2003; Coessmans et al., 2004). This form of LTP is mediated by the N-ethylmaleimide-sensitive factor (NSF)-dependent insertion of AMPARs into the postsynaptic membrane and dependent on presynaptically generated nitric oxide (NO) (Kakegawa and Yuzaki, 2005; Bouvier et al., 2016; Lev-Ram et al., 1997).

As with hippocampal LTP, PF-PC LTD is thought to require two distinct phases: early and late (Linden, 2012). Although little is known about the late phase, beyond a requirement for protein synthesis (Linden, 1996), the central engine driving the early phase of cerebellar LTD is a positive feedback loop that maintains PKC α activity for at least 20 min during LTD induction (Tanaka and Augustine, 2008; Linden and Connor, 1991; Antunes and De Schutter, 2012). To achieve sustained activity, PKC α activates the Ras-Raf-mitogen-activated protein kinase (MEK)-extracellular signal-regulated kinase (ERK) pathway, leading to the activation of cytosolic phospholipase A2 (cPLA2) (Lin et al., 1993; Tucker et al., 2009), which completes the loop by producing arachidonic acid, which maintains PKC activity (Shinomura et al., 1991; O’Flaherty et al., 2001). This positive feedback loop is heavily suppressed under basal conditions by a number of phosphatases, including protein phosphatase 1 (PP1) and protein phosphatase 2A (PP2A), to prevent spontaneous activation (Antunes and De Schutter, 2012; Ajima and Ito, 1995). Release of this suppression by inhibition of these phosphatases is as important for LTD expression as calcium activation of PKC α (Ajima and Ito, 1995; Ito, 2001). This phosphatase inhibition is driven primarily by Ca²⁺/calmodulin-dependent protein kinase II (CaMKII), activated by calcium-dependent calmodulin (CaM) (Chin and Means, 2000; Grabarek, 2005; Hansel et al., 2006). CaMKII behaves as an ultrasensitive switch that moves from very low basal activity to full activity within a very narrow calcium concentration range (Bradshaw et al., 2003; Kubota and Bower, 2001), making it an excellent candidate for the molecular source of the calcium threshold that determines whether LTP or LTD is generated by synaptic activity. As demonstrated by Kawaguchi and Hirano (2013), CaMKII gates LTD by negatively regulating phosphodiesterase 1 (PDE1) (Hashimoto et al., 1989; Kitagawa et al., 2009) and, thus, supports phosphatase inhibition by inhibiting the hydrolysis of cyclic guanosine monophosphate (cGMP).

Presynaptically generated NO has important roles in both PF-PC LTD and LTP: NO supports feedback loop activation during LTD induction by stimulating cGMP production via guanylyl cyclase (GC) and is both necessary and sufficient for LTP (Lev-Ram et al., 2002; Namiki et al., 2005; Kakegawa and Yuzaki,



2005), with NO scavengers fully preventing LTP (Kakegawa and Yuzaki, 2005; Bouvier et al., 2016). Unlike PF-PC LTD, NO does not act via GC during LTP induction because postsynaptic LTP is completely independent of the cGMP pathway (Lev-Ram et al., 2002). Rather, NO nitrosylates NSF, enhancing its ability to dismantle complexes of AMPAR and protein interacting with C kinase 1 (PICK-1), promoting reinsertion of AMPARs into the postsynaptic membrane (Huang et al., 2005; Hanley et al., 2002; Sossa et al., 2007). NO is sufficient for LTP regardless of its source and fully occludes 1-Hz-induced LTP (Lev-Ram et al., 2002). In both LTD and during the standard 1-Hz LTP protocol, the generation of NO is dependent on the retrograde transport of the postsynaptically generated cannabinoid 2-arachidonoylglycerol (2-AG) (Wang et al., 2014; Safo and Regehr, 2005). 2-AG, which can be synthesized from either diacylglycerol or arachidonic acid (AA) (Wang et al., 2014; Su et al., 2013), activates presynaptic CB1R receptors, leading to NO synthase (NOS) activation (Carney et al., 2009). CB1R couples to Gi/o (Carney et al., 2009; Howlett et al., 2010) and activates phosphatidylinositol 3-kinase (PI3K) (Sánchez et al., 2003; Stephens et al., 1997), leading to phosphatidylinositol (3,4,5)-trisphosphate (PIP3) production and phosphoinositide-dependent protein kinase-1 (PDK1) activation (Vanhaesebroeck and Waterfield, 1999). Activated PDK1 then activates the serine/threonine-specific protein kinase Akt (Jain and Bhalla, 2009; Gómez del Pulgar et al., 2000), which phosphorylates and activates NOS (Dimmeler et al., 1999; Lipina and Hundal, 2017). The role of the Akt pathway in NOS activation has previously been demonstrated in granule cells (Ciani et al., 2002).

Here we present a *trans*-synaptic model of bidirectional PF-PC plasticity (Figure 1) comprising 531 species, 376 reaction parameters, and 1,100 unidirectional reactions. A number of the key components of the network, including PKC, cPLA2, CaMKII, and the presynaptic cascade leading to NOS activation, were fully rebuilt to better reflect their true biochemical mechanism and behavior. As well as replicating both LTD and LTP, our model reveals an ultrasensitive “on switch” and an automatic “off switch” mechanism for the feedback loop, controlled by CaMKII and phosphatase activity. Together, these switches demarcate the beginning and end of the early phase of LTD expression. In addition, our model provides a molecular explanation for the differential roles of PP1 and PP2A in the regulation of LTD induction and reconciles conflicting experimental data regarding the importance of NO in cerebellar plasticity. Using PCs *in vitro*, we also establish the importance of the NSF-AMPA interaction and the strict frequency dependence of PF-PC LTP and, in combination with the results of our model simulations, reveal the mechanism behind this in terms of stimulation-dependent NO production. These results affirm the importance of coordination between pre- and postsynaptic signaling cascades in controlling bidirectional plasticity and uncover a possible *trans*-synaptic feedback loop regulating pre-synaptic NO production.

RESULTS

Simulated PF Stimulation Induces LTP, whereas Paired PF and CF Stimulation Induces LTD

The magnitude of depression achieved in experiments is dependent on the specific LTD/LTP induction protocol employed and

varies significantly between labs. Depression between 30% and 60% is typical (Tanaka et al., 2007; Matsuda et al., 2000), although depression of more than 65% is also possible (Launey et al., 2004). 1-Hz LTP typically produces a slower-building 20%–50% increase in synaptic efficacy (Lev-Ram et al., 2002).

A single PF stimulation was modeled with a 1-ms glutamate pulse (Doi et al., 2005) and a concurrent 1-ms Ca square pulse reaching ~200 nM (Doi et al., 2005). This PF-dependent Ca transient models the Ca influx through voltage-gated Ca channels activated via glutamate-AMPA-mediated local depolarization (Eilers et al., 1995; Finch et al., 2012). CF activity was modeled as a 2-ms square pulse of Ca, eliciting a maximum concentration of ~500 nM (Konnerth et al., 1992; Tanaka et al., 2007). When PF stimulation was paired with CF stimulation (100 stimulations at 1 Hz with a 100-ms delay between the PF and CF stimulations) (Chen and Thompson, 1995; Coesmans et al., 2004), the postsynaptic density (PSD) AMPAR population declined to ~60% of its baseline value over ~15 min (Figure 2A). However, PF stimulation alone (300 stimulations at 1 Hz) induced an ~30% increase in the PSD AMPAR population over ~60 min (Figure 2B). This potentiation was preceded by an initial decline in the AMPAR PSD population during PF stimulation. This initial depression is caused by transient calcium-mediated PKC activation during PF stimulation and can be observed in a number of experimental studies of LTP (e.g., Emi et al., 2013; Piochon et al., 2016; Bouvier et al., 2016). Whether LTD or LTP is expressed is largely dependent on whether the calcium surpasses the threshold for CaMKII activation. Our model includes a new 2-subunit CaMKII model that exhibits the crucial ultrasensitive switching behavior, as observed experimentally (Bradshaw et al., 2003; Figure 2C).

The Positive Feedback Loop Automatically Deactivates after the Early Phase of LTD Induction

Following the LTD induction protocol, ERK is rapidly phosphorylated, and this phosphorylation is maintained, indicating sustained activation of the feedback loop and coinciding with a strong inhibition of PP2A. However, ~40 min following LTD induction, ERK is rapidly and completely dephosphorylated, indicating the loop's spontaneous deactivation (Figure 3A). The other loop components also follow this pattern of activation (Figure 3B). This ERK dephosphorylation is initiated shortly after the complete inactivation of CaMKII (Figure 3A) and during a rebound of PP2A activity. This suggests that inhibition of phosphatase activity by CaMKII disinhibits the feedback loop, gating its activation, as reported previously (Kawaguchi and Hirano, 2013). However, after CaMKII is fully dephosphorylated, the rebound in phosphatase activity again inhibits the loop, causing it to deactivate (Figure 3C).

NO Supports LTD Induction by Facilitating Positive Feedback Loop Activation but Is Not Required with Strong Calcium Signals

During our simulated LTD protocol, NO facilitates sustained activation of the postsynaptic feedback loop and LTD expression (Figures 4A and 4B). However, if NO generation is blocked, then the positive feedback loop fails to activate, and LTD is not expressed; although the PSD AMPAR population initially declines, this is not maintained, and it returns to baseline

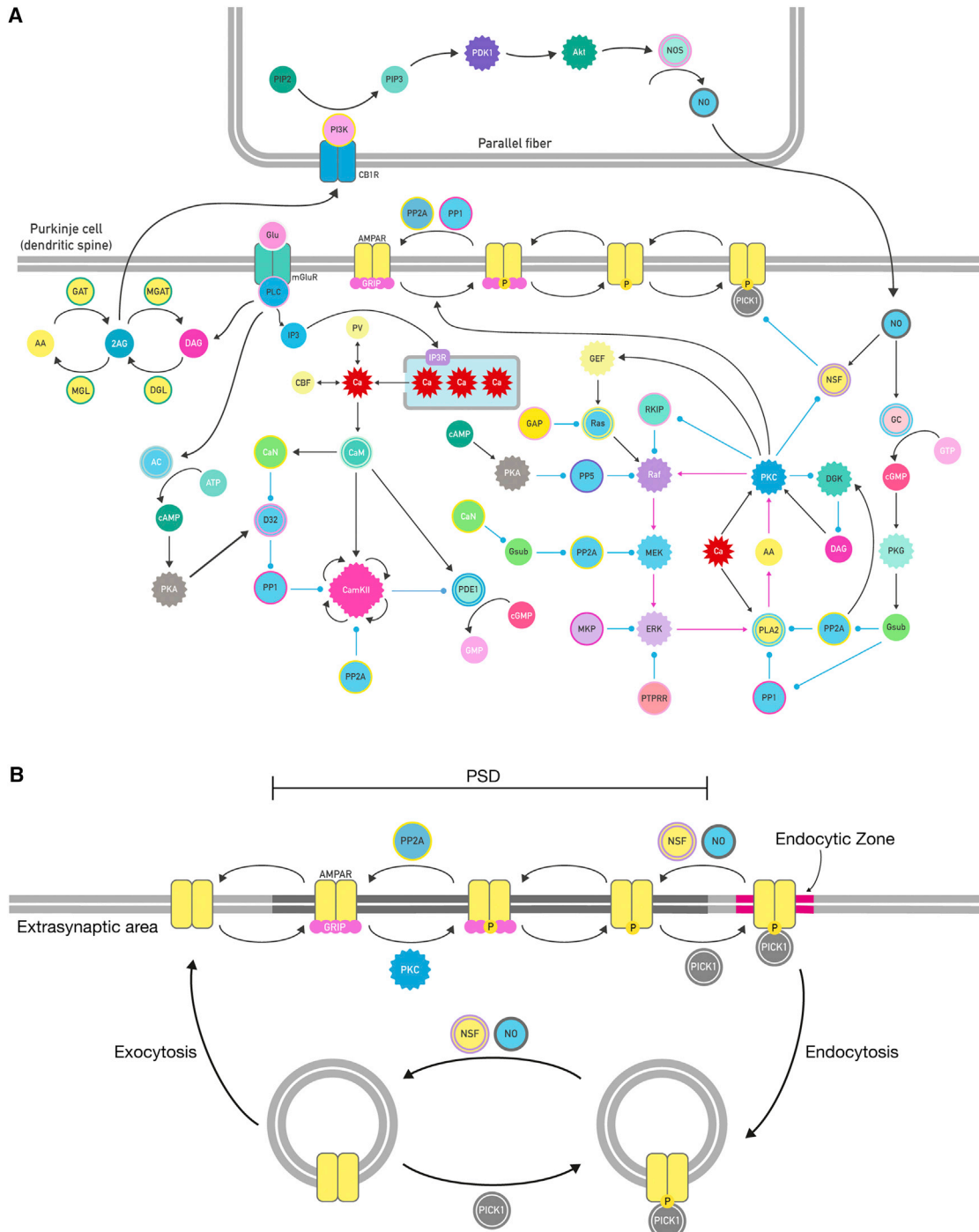


Figure 1. The Molecular Network Regulating PF-PC LTP and LTD

(A) Intracellular molecular network model, including both presynaptic and postsynaptic signaling cascades.

(B) AMPAR trafficking model, including regulation of AMPAR mobility by serine phosphorylation and exocytosis regulation by NO/NSF.

(Figures 4A and 4B). However, if the strength of the calcium transient is increased (e.g., by a square pulse at 5 μ M for 10 s), then the activation of the feedback loop is maintained for \sim 30 min, and LTD is successful (Figures 4B and 4C). This suggests that NO is supporting the activation of the feedback loop when the

calcium transient is weak but is not necessary when calcium levels are more elevated and/or sustained, as might be achieved during calcium uncaging protocols. Experiments have shown that deletion of either α -CaMKII (Hansel et al., 2006) or β -CaMKII (van Woerden et al., 2009) abolishes LTD and converts LTD to

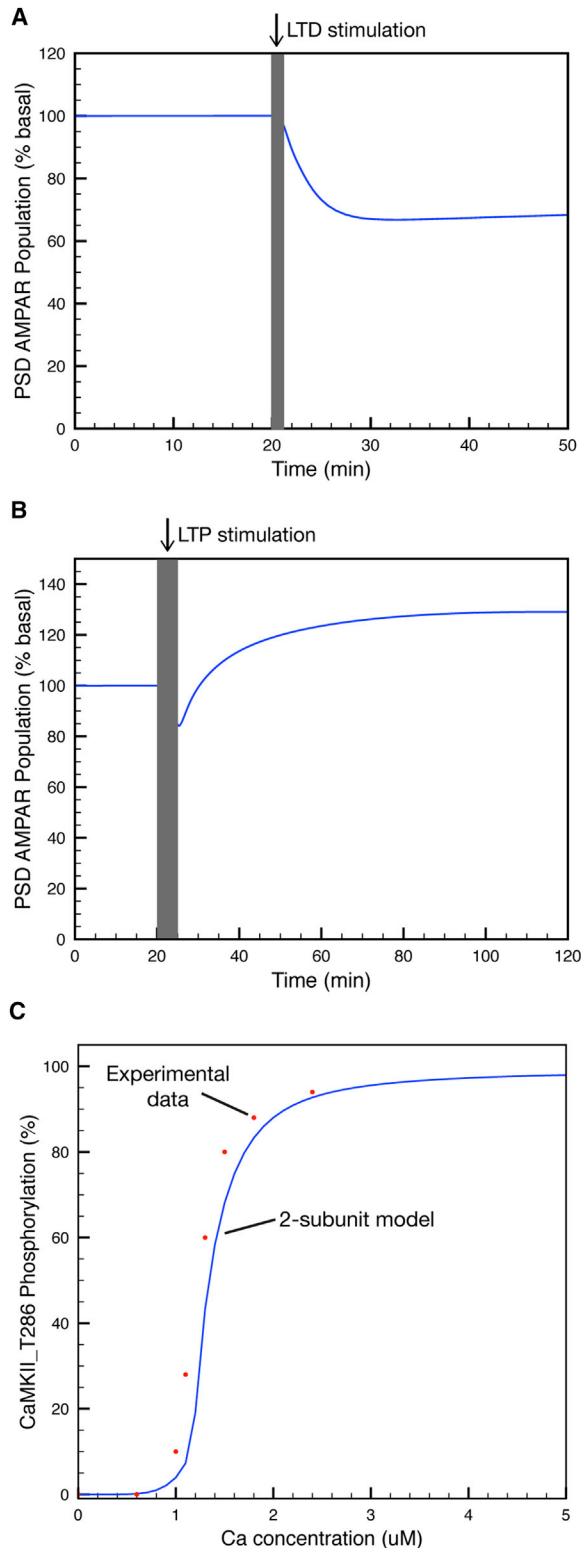


Figure 2. Induction of LTD and LTP in the Model Simulation
 (A) LTD is induced by concurrent PF (5 pulses, 100 Hz) and CF (1 pulse with 100-ms delay) stimulation.
 (B) LTP is induced by PF stimulation alone (300 pulses, 1 Hz).

LTP. We were able to replicate this effect by removing CaMKII from the model (Figure 4D).

Phosphatase Activity Suppresses the Feedback Loop under Basal Conditions and Regulates Its Activation and Inactivation

To explore the role of phosphatase activity in suppressing spontaneous activation of the feedback loop under basal conditions, we selectively inhibited either PP1 or PP2A from 20 min during basal recycling. Inhibition of PP1 had no effect, whereas sustained inhibition of PP2A resulted in an ~30% reduction of the PSD AMPAR population over 30 min (Figure 5A). This depression resulted from the spontaneous and sustained activation of the feedback loop independent of CaMKII activity, indicated by sustained phosphorylation of ERK and PKC activation (Figure 5B). Because the feedback loop off switch is normally dependent on the rebound of phosphatase activity following CaMKII deactivation, the feedback loop remains active indefinitely under these conditions. Inhibition of PP1, however, failed to cause loop activation. Similarly, inhibition of either PP5 or MAP kinase phosphatase (MKP) had no effect, indicating that PP2A has the primary role in suppressing the feedback loop under basal conditions. However, varying the concentration of PP1 (50%, 100%, 200%, and 400% of the wild-type concentration) revealed a role in regulating the activation and deactivation of the feedback loop, with lower concentrations delaying loop inactivation and higher concentrations blocking activation entirely (Figure 5C). Reducing the PP1 concentration below 50% of the wild-type concentration had no significant additional effect on loop inactivation, indicating that PP2A is the primary phosphatase in driving loop inactivation, with PP1 providing a supporting regulatory role.

1-Hz LTP Requires the Interaction between NSF and GluA2

It has been reported previously that LTP is triggered by the application of an NO donor at the PF-PC synapse and that NSF-dependent insertion of GluA2-containing AMPARs into synapses mediates this form of LTP (Kakegawa and Yuzaki, 2005). To test whether LTP triggered by 1-Hz PF stimulation also relies on the NSF-GluA2 interaction, we added a peptide that interferes with the interaction, pep2m (Noel et al., 1999; Lüthi et al., 1999), to the internal solution during LTP induction. The amplitudes of excitatory postsynaptic currents evoked by PF stimulation (PF-EPSCs) were normalized immediately prior to LTP induction. In the presence of pep2m, PF-EPSC amplitudes were decreased around 30–40 min after establishing a whole-cell configuration, and a further slight reduction of PF-EPSC was observed after 1-Hz PF stimulation (Figure 6A). This reduction in EPSC in the presence of pep2m is likely a result of compromised exocytosis and could be replicated in our simulations. In contrast, when a control peptide (pep4c) was used, basal PF-EPSCs were not affected, and LTP was successfully induced by 1-Hz PF stimulation (Figure 6A). The amplitudes calculated 20–30 min after PF

(C) Ultrasensitive activation of CaMKII with calcium concentration. Shown is a comparison of 2-subunit CaMKII model and experimental data (Bradshaw et al., 2003).

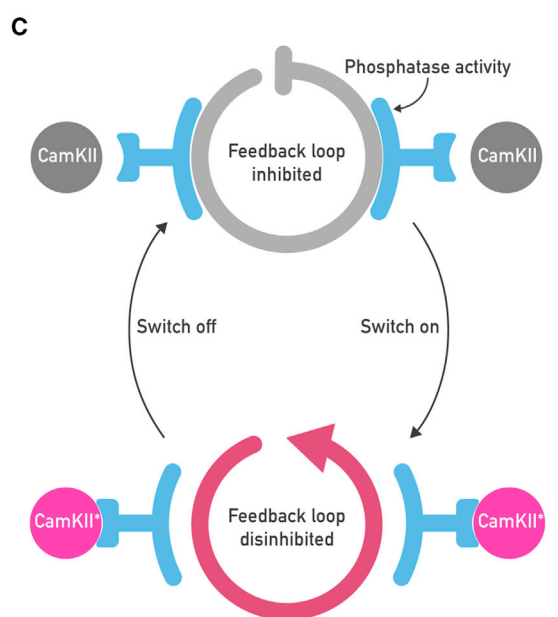
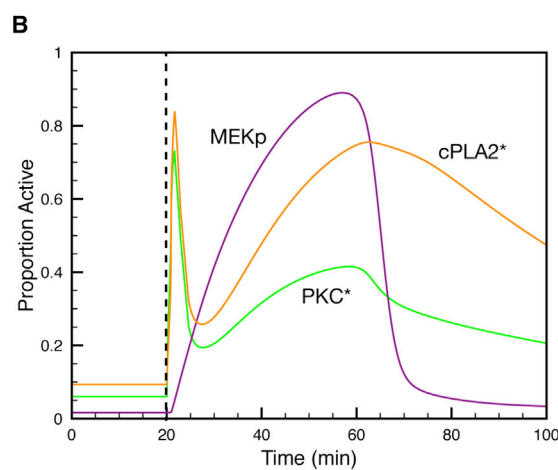
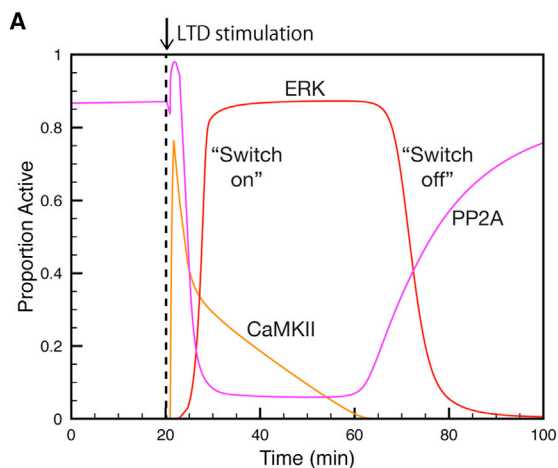


Figure 3. Time Course of Feedback Loop Components during LTD Induction

(A) Time courses of active PP2A and phosphorylated CaMKII and ERK during the early phase of LTD induction.

(B) Time courses of PKC, MEK, and cPLA2 activation during the early phase of LTD induction.

(C) The feedback loop is highly excitable and requires constant basal suppression by phosphatase activity to avoid spontaneous activation. Activated CaMKII (CaMKII*) suppresses phosphatase activity, removing the “brakes” from the loop, leading to rapid and sustained activation. CaMKII deactivation later causes a rebound in phosphatase activity that switches off the loop.

stimulation were significantly smaller in the presence of pep2m than those in the presence of pep4c. These results suggest that LTP triggered by 1-Hz PF stimulation is mediated by NSF-dependent insertion of AMPARs into synapses.

LTP Induction in PCs Has a Strict Frequency Dependence

Previous studies have shown that postsynaptically expressed LTP can be triggered at PF-PC synapses by 300 PF pulses at 1 Hz (Lev-Ram et al., 2002; Coesmans et al., 2004; Belmeguenai and Hansel, 2005), but the frequency dependence of LTP has not been studied more systematically. We confirmed the LTP induction by the 1-Hz PF stimulation protocol (Figures 6B and 6C). Consistent with previous reports, the LTP was expressed postsynaptically because paired pulse facilitation (PPF) ratios were not altered by the stimulation (see Fig. S1). To test the frequency dependence of LTP induction, 0.5- or 0.67-Hz (2 or 1.5 s between stimuli) PF stimulation was applied instead of 1-Hz stimulation. However, neither frequency of stimulation was successful in triggering LTP. In addition, even when 0.5-Hz stimulation was applied 600 times, LTP was not triggered. The averaged PF-EPSC amplitudes calculated at 20–30 min after 1-Hz stimulation was significantly different from those after 0.5- or 0.67-Hz stimulation (Figures 6B and 6C). Thus, it seems that there is a threshold of PF stimulation frequency for triggering LTP and that the threshold is higher than the resting firing frequency of granule cells (Powell et al., 2015; Chen et al., 2017; Chadderton et al., 2004).

The Postsynaptic Feedback Loop Is Nested within a trans-Synaptic Feedback Loop Controlling NO Production

In agreement with our experimental observations and others (Lev-Ram et al., 2002), 100 PF pulses at 1 Hz was insufficient to elicit LTP in our model simulations, as was 300 pulses at either 0.5 or 0.67 Hz (Figure 6D). These LTP induction conditions are unsuccessful because they fail to induce sufficient levels of NO in the postsynaptic cytosol, with the NO concentration remaining below 0.07 μM , whereas 300 pulses at 1 Hz induce a NO spike reaching 0.21 μM (Figure 6E). This train of PF stimuli induces cPLA2 activation, via Ca, that is maintained throughout the stimulation period but rapidly drops off when stimulation ends (Figure 6F). Thus, the production of NO during PF stimulation is entirely stimulation-dependent: NO is only produced and accumulates during stimulation and immediately begins to decline after the stimulation period. In contrast, during LTD induction, NO continues to rise to $\sim 0.35 \mu\text{M}$ post-induction before slowly

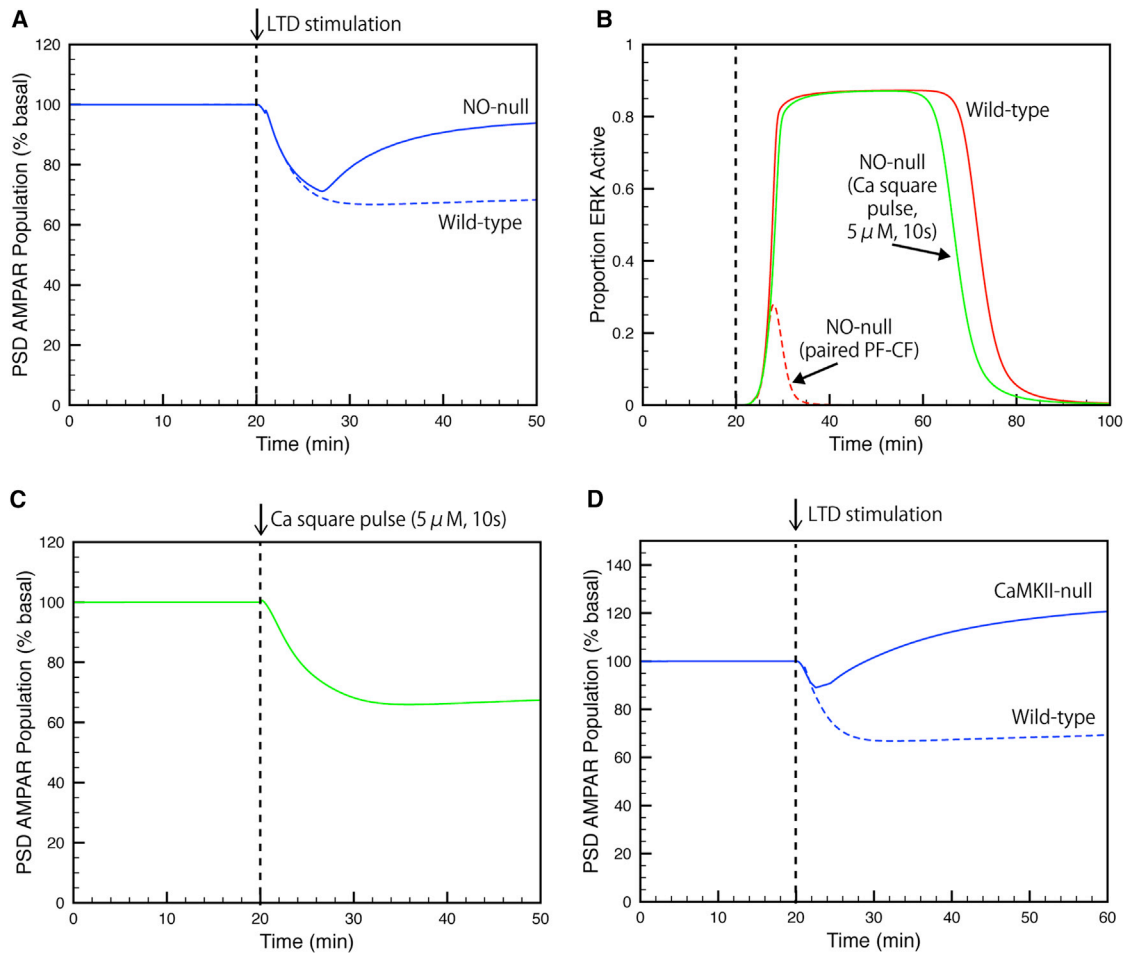


Figure 4. NO and CaMKII (via PDE1) Cooperate to Support Feedback Loop Activation

(A) Blocking NO production causes the initial reduction in PSD AMPAR population to revert toward basal levels.

(B) Failure of LTD when NO is blocked is caused by a failure of sustained postsynaptic feedback loop activation, reported as active ERK. However, a strong calcium signal can obviate the requirement for NO and induce sustained loop activation even in its absence.

(C) Even in the absence of NO, a strong calcium signal (5 μ M for 10 s) can successfully induce LTD.

(D) Removal of CaMKII from the model causes conversion of LTD to LTP.

declining (Figure 7A). This result uncovers a possible *trans*-synaptic feedback loop responsible for maintaining high NO levels during LTD induction (Figure 7B).

DISCUSSION

The default response to increased PF stimulation at PCs is LTP because calcium levels remain below the threshold for CaMKII activation but become high enough to activate cPLA2 and stimulate the production of 2-AG via AA (Wang et al., 2014; Su et al., 2013). This explains why deletion of CaMKII converts LTD to LTP under LTD induction conditions (van Woerden et al., 2009); the network driving LTD is only activated when CaMKII is activated. In the absence of CaMKII, potentiation is the default response to PF stimulation, whether alone or accompanied by concurrent CF stimulation. Our model simulations were able to replicate this important effect. Although β -CaMKII-null mice also exhibit a

switch in the opposite direction, from LTP to LTD under LTP induction conditions, this is caused by the extraneous activation of α -CaMKII rather than any particularly interesting network effect (van Woerden et al., 2009). Because PF activity is a unilateral driver of LTP, we predicted a sharp threshold for LTP induction above the PF resting firing rate of 0.1–0.5 Hz (Chadderton et al., 2004; Chen et al., 2017; Powell et al., 2015), which our experiments in PCs were able to demonstrate. Our model simulations revealed that subthreshold PF stimulation frequencies fail to induce sufficient NO to trigger LTP; the production of NO during LTP induction is entirely dependent on continuous PF stimulation at a suprathreshold frequency, with NO levels building during stimulation but dropping off as soon as stimulation ends.

CaMKII activation, as a result of suprathreshold calcium increase, acts as the switch from the default LTP to LTD (van Woerden et al., 2009). CaMKII suppresses phosphatase activity, leading to the disinhibition and activation of the postsynaptic

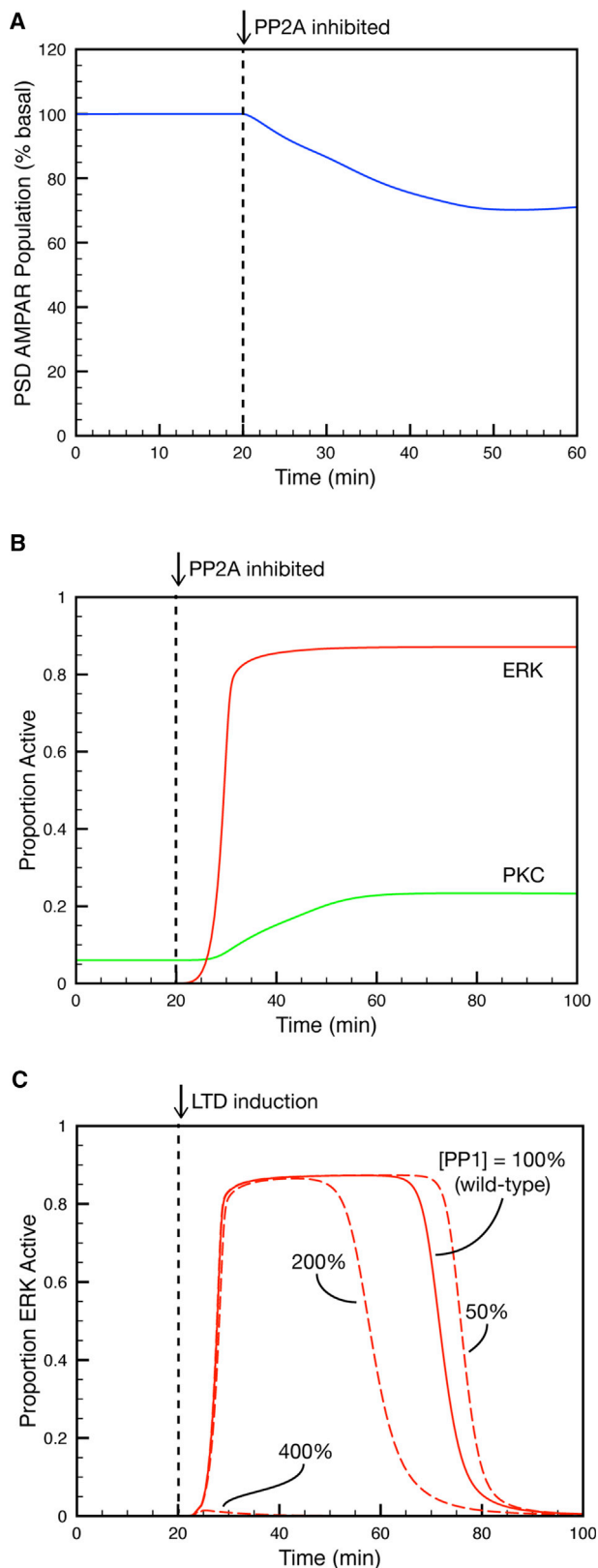


Figure 5. Phosphatase Regulation of Feedback Loop Activation and Deactivation

(A) Sustained inhibition of PP2A induces LTD.
 (B) Sustained inhibition of PP2A induces feedback loop activation, indicated by sustained ERK phosphorylation and PKC activation.
 (C) Effect of PP1 inhibition on loop activation and inactivation following the LTD induction protocol. PP1 regulates loop activation, with increasing levels of active PP1 reducing the time during which the loop is active or blocking activation entirely.

positive feedback loop that sustains PKC activity. The critical role of this feedback loop in driving early PF-PC LTD is well-established (Tanaka et al., 2007; Tanaka and Augustine, 2008), and our model reveals how CaMKII acts as the ultrasensitive on-switch (Bradshaw et al., 2003) for this loop. In previously published models of cerebellar plasticity, when activated, the loop remains active indefinitely, with no known mechanism of deactivation. However, experiments show that active PKC is no longer required beyond the early phase of LTD (Tanaka and Augustine, 2008; Tsuruno and Hirano, 2007). PKC inhibitors applied shortly after LTD induction cause the EPSC to recover and LTD to fail, but inhibition of PKC, when depression has reached its maximal level, has no effect on its maintenance (Tanaka and Augustine, 2008). It thus makes sense that the feedback loop ought to deactivate after the early phase of LTD induction is complete. Congruent with these experimental observations, our model reveals a rapid and automatic off-switch for the feedback loop that defines the end of the early phase of LTD and heralds entry into the late phase.

This off-switch is driven by the rebound in phosphatase activity following CaMKII inactivation. Under basal conditions, these phosphatases actively suppress the key components of the feedback loop and prevent its spontaneous activation. Indeed, PP2A inhibition alone will elicit robust PF-PC LTD (Launey et al., 2004), presumably resulting from spontaneous loop activation, in addition to unopposed AMPAR-GluA2-S880 phosphorylation (Kohda et al., 2013; Gallimore et al., 2016). Inhibition of PP1, in contrast, has no effect (Launey et al., 2004). We were able to replicate these experimental results and explain the differential effects of PP1 and PP2A inhibition: removal of PP2A during basal AMPAR recycling resulted in significant depression in our model simulation, whereas removal of PP1 had no effect. This is because only PP2A removal caused the feedback loop to spontaneously activate, independent of CaMKII, indicating that PP2A is the primary phosphatase in basal suppression of the loop, specifically by suppressing MEK and cPLA2 activity, with other phosphatases, such as PP1 and calcineurin, supporting the role of PP2A. This result contrasts with Belmeguenai and Hansel (2005), who did not observe spontaneous LTD by PP2A inhibition alone in cerebellar slice preparations. However, PP2A inhibition resulted in significant depression under LTP induction conditions, indicating that PF stimulation was required to activate the PKC feedback loop under their experimental conditions. These contrasting experimental results might suggest that the balance of phosphatase activity is variable under differing physiological conditions and might be regulated by still unknown mechanisms. These complex effects of phosphatase activity on the feedback loop are further complicated by the observation that the calcium threshold for CaMKII activation

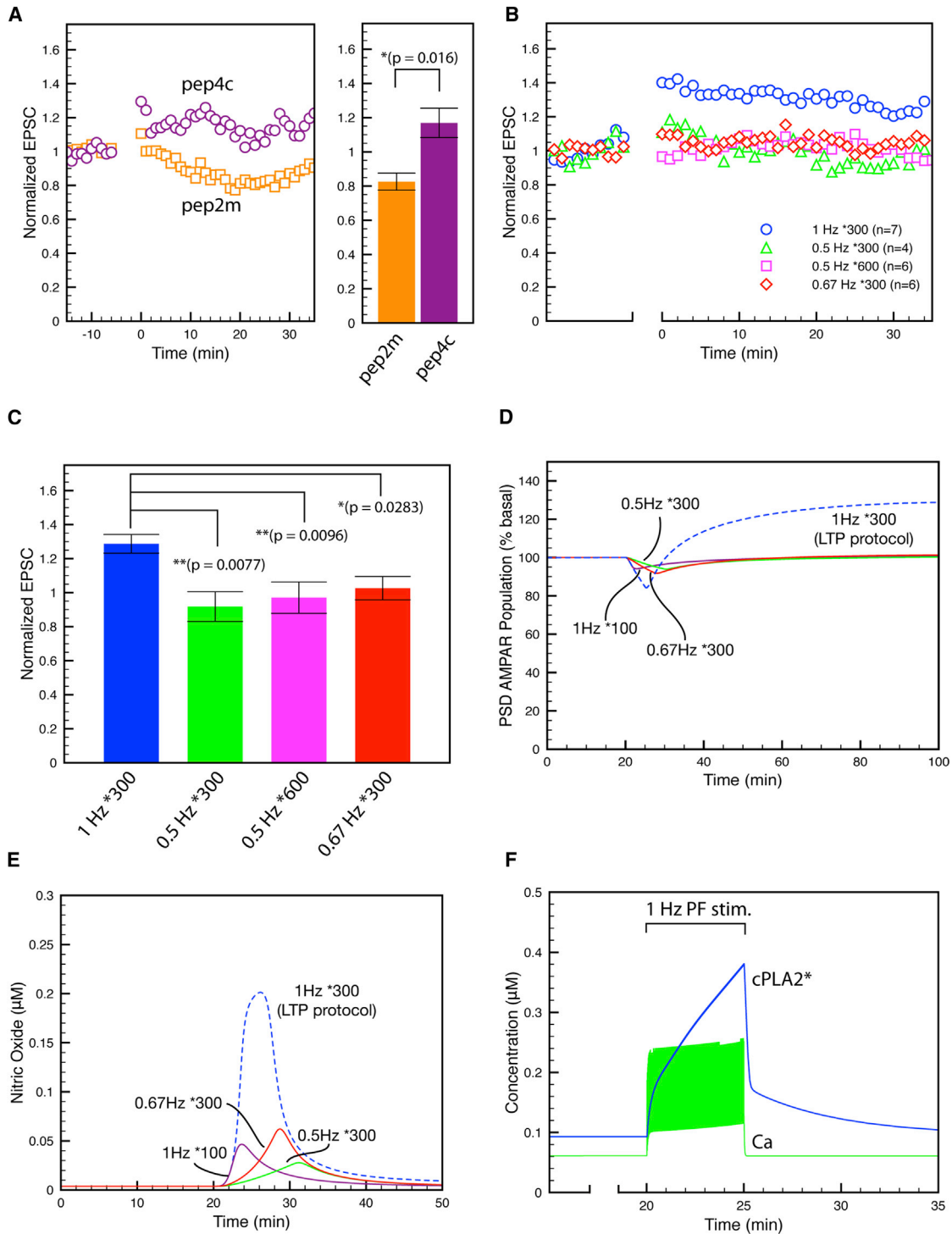


Figure 6. LTP Is Mediated by the NSF Interaction with GluA2 AMPARs and Is Triggered by 1-Hz but Not 0.5- or 0.67-Hz PF stimulation

(A) Time course of changes in PF-EPSCs in the presence of pep2m ($n = 5$) or pep4c ($n = 5$). The 1-Hz PF stimulation triggered LTP in the presence of pep4c but not in the presence of pep2m. PF-EPSC amplitudes are normalized to their mean prestimulation levels. The histogram shows mean (\pm SEM) PF-EPSC amplitudes 20–30 min after PF stimulation. * $p < 0.05$.

(B) Time course of changes in PF-EPSCs after a different frequency of PF stimulation. LTP was triggered by 300 PF stimulation at 1 Hz ($n = 7$) but not by 300 ($n = 4$) or 600 ($n = 6$) PF stimulation at 0.5 Hz or 300 PF stimulation at 0.67 Hz ($n = 6$).

(C) Averaged PF-EPSC amplitudes calculated 20–30 min after PF stimulation.

(legend continued on next page)

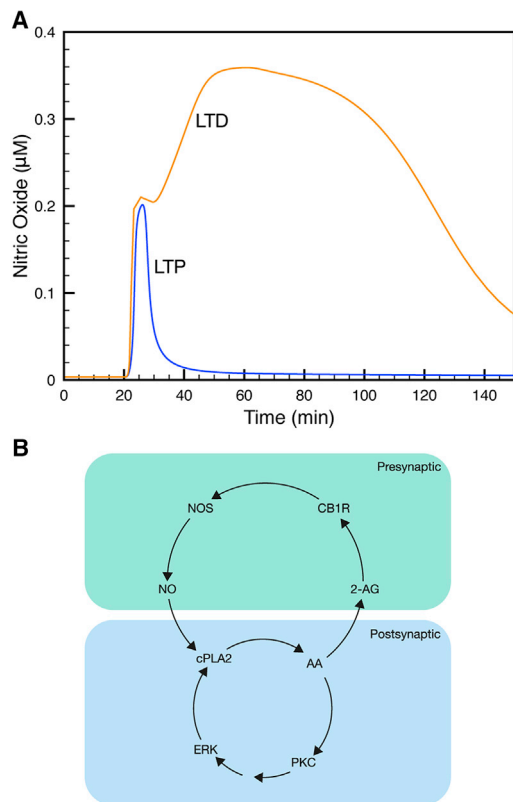


Figure 7. A *trans*-Synaptic Positive Feedback Loop Regulates LTP and LTD

(A) LTP induction is accompanied by stimulus-dependent NO generation that declines immediately after the PF stimulation ends. However, LTD induction generates sustained increases in NO.

(B) A *trans*-synaptic feedback loop, within which the postsynaptic PKC loop is nested, produces sustained increases in NO throughout LTD induction. This loop is driven by retrograde 2-AG activation of presynaptic CB1R, leading to NOS activation.

can itself shift as a result of inhibitory T305 autophosphorylation, depending on the frequency of PF stimulation. This threshold shift to higher calcium concentrations during high-frequency PF stimulation allows the CF signal to remain instructive in LTD induction over a wide range of PF stimulation frequencies (Piochon et al., 2016).

Although NO-mediated activation of the cGMP/PKG pathway undoubtedly supports phosphatase inhibition, it remains a matter of debate as to whether NO provides an indispensable or supporting role in LTD induction. Although PF-PC LTD was found to be absent in mice and rats lacking neuronal NO synthase (Boxall and Garthwaite, 1996; Lev-Ram et al., 1997), LTD induction protocols using calcium uncaging alone are well-established (Tanaka et al., 2007). A recent study posited

that NO supports LTD induction when the calcium pulse is marginally supra-threshold or transient but unnecessary when the calcium concentration is high or sustained (Bouvier et al., 2016). This makes sense because calcium uncaging protocols are able to rapidly discharge large quantities of calcium into the cytosol that are more likely to reach high and sustained levels, obviating the requirement for elevated NO. However, under normal physiological conditions, the relatively weak calcium signal generated by paired PF and CF activity fails to generate sustained CaMKII activity. Under these conditions, concurrent activation of the presynaptic NOS pathway is required to augment CaMKII-mediated phosphatase inhibition. These results are congruent with and extend those of Kawaguchi and Hirano (2013), who showed previously that CaMKII and NO cooperate in releasing the feedback loop from phosphatase suppression during LTD induction.

Given that LTP is driven by a low postsynaptic calcium concentration below the LTD threshold, it is perhaps surprising that calcium uncaging protocols fail to induce LTP under low-calcium conditions. Although the presynaptic terminals responsible for NO production are present and, presumably, functional in cerebellar slice preparations, neither LTP nor LTD is triggered below the threshold for CaMKII activation in these uncaging protocols (Tanaka et al., 2007). However, our model resolves this apparent anomaly by revealing how LTP is dependent on the sustained activation of cPLA2 by repeated PF stimulation (and, thus, calcium elevation) over several minutes, whereas uncaging protocols typically increase calcium for only a few seconds. 1-Hz PF stimulation over 5 min maintains cPLA2 activity and generates a large, entirely stimulation-dependent increase in postsynaptic NO. If the frequency of PF stimulation is below the 1 Hz threshold, or if the number of pulses is below 300, then insufficient NO is generated, and LTP fails. In contrast to this stimulation-dependent NO spike during LTP induction, our model simulations reveal sustained NO production during LTD induction long after the PF-CF stimulation ends. This suggests that the postsynaptic PKC feedback loop is nested within a larger *trans*-synaptic positive feedback loop that maintains NOS activity and, thus, NO production during the entire early phase of LTD. Because NO has a crucial role in supporting loop activation by the activation of GC and because GC deactivates within seconds of NO removal (Newton et al., 2010; Bellamy and Garthwaite, 2001), it is plausible that sustained NO levels help to prevent the premature inactivation of the postsynaptic PKC feedback loop. In contrast, because LTP relies on the nitrosylation of NSF, and the half-life of nitrosylated proteins in plasma is typically at least 40 min (Stamler et al., 1992), the sustained production of NO throughout LTP induction is not required. In our model, nitrosylated NSF has a half-life of around 50 min, which is in line with experiments showing that NSF is denitrosylated within 3 hr following nitrosylation (Ito et al., 2011) but with a sufficient lifetime for LTP to be fully expressed.

(D) LTP induction in our model simulations requires 300 pulses at 1 Hz. 100 pulses at 1 Hz are not sufficient to induce LTP. Likewise, 300 pulses at either 0.5 or 0.67 Hz fail to induce LTP.

(E) Only 300 pulses at 1 Hz generate high levels of NO, with lower pulse frequencies or numbers failing to generate NO levels above 0.07 μ M.

(F) PF stimulation at 1 Hz for 5 min elevates and maintains cPLA2 activity throughout this period by repeated Ca spikes. This allows AA and, thus, 2-AG to accumulate, leading to the activation of presynaptic NOS and NO production.

EXPERIMENTAL PROCEDURES

All procedures involving mice were performed according to the guidelines of the Institutional Animal Care and Use Committee of the Korea Institute of Science and Technology.

Fresh sagittal slices of the cerebellum were prepared from 21- or 22-day-old C57BL/6 mice of either sex. Slices were bathed in artificial cerebrospinal fluid (ACSF) containing 125 mM NaCl, 2.5 mM KCl, 1.3 mM MgCl₂, 2 mM CaCl₂, 1.25 mM NaH₂PO₄, 26 mM NaHCO₃, 20 mM glucose, and 0.01 mM bicuculline methochloride (Tocris Bioscience). Patch pipettes (resistance, 5–9 MΩ) were filled with 130 mM potassium gluconate, 2 mM NaCl, 4 mM MgCl₂, 4 mM Na₂-ATP, 0.4 mM Na-GTP, 20 mM HEPES (4-(2-hydroxyethyl)-1-piperazineethanesulfonic acid) (pH 7.2), and 0.5 EGTA. For the experiments using peptide, pep2m or pep4c (200 μM, Tocris Bioscience) along with Alexa 568 (125 μM, Thermo Fisher Scientific) was included in the internal solution.

Patch-Clamp Recording

Whole-cell patch-clamp recordings were made from PCs in cerebellar sagittal slices that were visually identified under a microscope (Olympus BX61WI or Nikon FN1). PFs were activated to evoke PF-EPSCs in PCs (holding potential of −70 mV) with a glass stimulating electrode on the surface of the molecular layer. PF-EPSCs were acquired and analyzed using pClamp software (Molecular Devices). To measure the PPF ratios, PF-EPSCs were evoked by a pair of PF stimulations with a 100-ms interval. LTP was triggered by 300 PF stimulations at 1 Hz. To test the frequency dependence, the PF stimulation was applied 300 or 600 times at 0.5 or 0.67 Hz. Data were accepted when the series resistance changed by <30%, the input resistance was >70 megaohms (MΩ) and the holding current changed by <20%. The criteria were pre-established. When pep2m or pep4c was included in the internal solutions, recording was started around 30 min after establishing the whole-cell configuration and continued for another 30 min before applying 1-Hz PF stimulation to allow the peptide to diffuse into the recording PCs.

Statistical Analysis

The sampling distribution was not tested because of small sample numbers. Instead, statistical differences were determined by Mann-Whitney test (for two-group comparisons) and one-way ANOVA followed by uncorrelated Fisher's least significant difference (LSD) test (for more than two-group comparisons), which does not require normal distribution and is not very sensitive to deviations from normality, respectively. Analyses were performed using GraphPad Prism 6 and OriginPro software for a statistical significance level of $p < 0.05$. n represents the number of cells recorded.

Model Background and Construction

The complete differential equation model (ModelDB: 235376) was built in a modular fashion, consisting of a single well-mixed compartment containing seven integrated modules (in addition to other regulatory components; Figure 1):

- (1) AMPAR trafficking model
- (2) Calcium model, including metabotropic glutamate receptor (mGluR) and inositol trisphosphate receptor (IP3R)
- (3) Postsynaptic positive feedback loop with phosphatase regulation
- (4) CaMKII model with regulatory components
- (5) NO/cGMP pathway
- (6) NO/NSF/PICK-1 model to implement LTP
- (7) Presynaptic cascade to activate NOS (via CB1R)

The complete model was implemented in the MATLAB Simbiology package using the ODE15s solver and comprised 531 species, 358 reaction parameters, and 1,120 individual reactions (Figure 1). A more detailed description of the model construction can be found in the Supplemental Experimental Procedures. All model species, parameters, and reactions are listed in Tables S1, S2, and S3, respectively.

Simulation of LTD and LTP Induction

We modeled PF stimulation with a 1-ms glutamate pulse combined with a 1-ms Ca square pulse reaching ~200 nM, and CF activity was modeled as a

10-ms square pulse of calcium, eliciting a maximum concentration of ~500 nM (Konnerth et al., 1992; Tanaka et al., 2007). To simulate LTP, the PSD AMPAR population was allowed to equilibrate for 20 min, and then 300 PF pulses alone were applied at 1 Hz (other frequencies were also explored, as discussed in the Results). LTD induction was simulated by applying 100 PF and CF pulses (concurrent but with a 100 ms delay) at 1 Hz.

SUPPLEMENTAL INFORMATION

Supplemental Information includes Supplemental Experimental Procedures, three figures, and three tables and can be found with this article online at <https://doi.org/10.1016/j.celrep.2017.12.084>.

ACKNOWLEDGMENTS

This work was funded by the Okinawa Institute of Science and Technology Graduate University and by the Korea Institute of Science and Technology Institutional Program (Project 2E26860).

AUTHOR CONTRIBUTIONS

A.R.G. and E.D.S. conceived and designed the study. A.R.G. built the computational model, performed the simulations, and analyzed the data. T.K. and K.T.-Y. designed the experimental work in PCs. T.K. performed the experimental work and analyzed the data. A.R.G. and T.K. wrote the manuscript. A.R.G., T.K., K.T.-Y., and E.D.S. edited and revised the manuscript. K.T.-Y. and E.D.S. acquired funding, provided resources, and supervised the study.

DECLARATION OF INTERESTS

The authors declare no competing interests.

Received: February 2, 2017

Revised: November 10, 2017

Accepted: December 22, 2017

Published: January 16, 2018

REFERENCES

- Ajima, A., and Ito, M. (1995). A unique role of protein phosphatases in cerebellar long-term depression. *Neuroreport* 6, 297–300.
- Antunes, G., and De Schutter, E. (2012). A stochastic signaling network mediates the probabilistic induction of cerebellar long-term depression. *J. Neurosci.* 32, 9288–9300.
- Bellamy, T.C., and Garthwaite, J. (2001). Sub-second kinetics of the nitric oxide receptor, soluble guanylyl cyclase, in intact cerebellar cells. *J. Biol. Chem.* 276, 4287–4292.
- Belmeguenai, A., and Hansel, C. (2005). A role for protein phosphatases 1, 2A, and 2B in cerebellar long-term potentiation. *J. Neurosci.* 25, 10768–10772.
- Bouvier, G., Higgins, D., Spolidoro, M., Carrel, D., Mathieu, B., Léna, C., Dieudonné, S., Barbour, B., Brunel, N., and Casado, M. (2016). Burst-Dependent Bidirectional Plasticity in the Cerebellum Is Driven by Presynaptic NMDA Receptors. *Cell Rep.* 15, 104–116.
- Boxall, A.R., and Garthwaite, J. (1996). Long-term depression in rat cerebellum requires both NO synthase and NO-sensitive guanylyl cyclase. *Eur. J. Neurosci.* 8, 2209–2212.
- Bradshaw, J.M., Kubota, Y., Meyer, T., and Schulman, H. (2003). An ultrasensitive Ca²⁺/calmodulin-dependent protein kinase II-protein phosphatase 1 switch facilitates specificity in postsynaptic calcium signaling. *Proc. Natl. Acad. Sci. USA* 100, 10512–10517.
- Carney, S.T., Lloyd, M.L., MacKinnon, S.E., Newton, D.C., Jones, J.D., Howlett, A.C., and Norford, D.C. (2009). Cannabinoid regulation of nitric oxide synthase I (nNOS) in neuronal cells. *J. Neuroimmune Pharmacol.* 4, 338–349.
- Chadderton, P., Margrie, T.W., and Häusser, M. (2004). Integration of quanta in cerebellar granule cells during sensory processing. *Nature* 428, 856–860.

- Chen, C., and Thompson, R.F. (1995). Temporal specificity of long-term depression in parallel fiber–Purkinje synapses in rat cerebellar slice. *Learn. Mem.* **2**, 185–198.
- Chen, S., Augustine, G.J., and Chadderton, P. (2017). Serial processing of kinematic signals by cerebellar circuitry during voluntary whisking. *Nat. Commun.* **8**, 232.
- Chin, D., and Means, A.R. (2000). Calmodulin: a prototypical calcium sensor. *Trends Cell Biol.* **10**, 322–328.
- Chung, H.J., Steinberg, J.P., Hugarir, R.L., and Linden, D.J. (2003). Requirement of AMPA receptor GluR2 phosphorylation for cerebellar long-term depression. *Science* **300**, 1751–1755.
- Ciani, E., Virgili, M., and Contestabile, A. (2002). Akt pathway mediates a cGMP-dependent survival role of nitric oxide in cerebellar granule neurones. *J. Neurochem.* **81**, 218–228.
- Coesmans, M., Weber, J.T., De Zeeuw, C.I., and Hansel, C. (2004). Bidirectional parallel fiber plasticity in the cerebellum under climbing fiber control. *Neuron* **44**, 691–700.
- Dimmeler, S., Fleming, I., Fisslthaler, B., Hermann, C., Busse, R., and Zeiher, A.M. (1999). Activation of nitric oxide synthase in endothelial cells by Akt-dependent phosphorylation. *Nature* **399**, 601–605.
- Doi, T., Kuroda, S., Michikawa, T., and Kawato, M. (2005). Inositol 1,4,5-trisphosphate-dependent Ca²⁺ threshold dynamics detect spike timing in cerebellar Purkinje cells. *J. Neurosci.* **25**, 950–961.
- Eilers, J., Augustine, G.J., and Konnerth, A. (1995). Subthreshold synaptic Ca²⁺ signalling in fine dendrites and spines of cerebellar Purkinje neurons. *Nature* **373**, 155–158.
- Emi, K., Kakegawa, W., Miura, E., Ito-Ishida, A., Kohda, K., and Yuzaki, M. (2013). Reevaluation of the role of parallel fiber synapses in delay eyeblink conditioning in mice using Cbln1 as a tool. *Front. Neural Circuits* **7**, 180.
- Finch, E.A., Tanaka, K., and Augustine, G.J. (2012). Calcium as a trigger for cerebellar long-term synaptic depression. *Cerebellum* **11**, 706–717.
- Gallimore, A.R., Aricescu, A.R., Yuzaki, M., and Calinescu, R. (2016). A Computational Model for the AMPA Receptor Phosphorylation Master Switch Regulating Cerebellar Long-Term Depression. *PLoS Comput. Biol.* **12**, e1004664.
- Gómez del Pulgar, T., Velasco, G., and Guzmán, M. (2000). The CB1 cannabinoid receptor is coupled to the activation of protein kinase B/Akt. *Biochem. J.* **347**, 369–373.
- Grabarek, Z. (2005). Structure of a trapped intermediate of calmodulin: calcium regulation of EF-hand proteins from a new perspective. *J. Mol. Biol.* **346**, 1351–1366.
- Hanley, J.G., Khatri, L., Hanson, P.I., and Ziff, E.B. (2002). NSF ATPase and alpha-/beta-SNAPs disassemble the AMPA receptor-PICK1 complex. *Neuron* **34**, 53–67.
- Hansel, C., de Jeu, M., Belmeguenai, A., Houtman, S.H., Buitendijk, G.H.S., Andreev, D., De Zeeuw, C.I., and Elgersma, Y. (2006). alphaCaMKII is essential for cerebellar LTD and motor learning. *Neuron* **51**, 835–843.
- Hashimoto, Y., Sharma, R.K., and Soderling, T.R. (1989). Regulation of Ca²⁺/calmodulin-dependent cyclic nucleotide phosphodiesterase by the autophosphorylated form of Ca²⁺/calmodulin-dependent protein kinase II. *J. Biol. Chem.* **264**, 10884–10887.
- Howlett, A.C., Blume, L.C., and Dalton, G.D. (2010). CB(1) cannabinoid receptors and their associated proteins. *Curr. Med. Chem.* **17**, 1382–1393.
- Huang, Y., Man, H.Y., Sekine-Aizawa, Y., Han, Y., Juluri, K., Luo, H., Cheah, J., Lowenstein, C., Hugarir, R.L., and Snyder, S.H. (2005). S-nitrosylation of N-ethylmaleimide sensitive factor mediates surface expression of AMPA receptors. *Neuron* **46**, 533–540.
- Ito, M. (2001). Cerebellar long-term depression: characterization, signal transduction, and functional roles. *Physiol. Rev.* **81**, 1143–1195.
- Ito, T., Yamakuchi, M., and Lowenstein, C.J. (2011). Thioredoxin increases exocytosis by denitrosylating N-ethylmaleimide-sensitive factor. *J. Biol. Chem.* **286**, 11179–11184.
- Jain, P., and Bhalla, U.S. (2009). Signaling logic of activity-triggered dendritic protein synthesis: an mTOR gate but not a feedback switch. *PLoS Comput. Biol.* **5**, e1000287.
- Kakegawa, W., and Yuzaki, M. (2005). A mechanism underlying AMPA receptor trafficking during cerebellar long-term potentiation. *Proc. Natl. Acad. Sci. USA* **102**, 17846–17851.
- Kawaguchi, S.Y., and Hirano, T. (2013). Gating of long-term depression by Ca²⁺/calmodulin-dependent protein kinase II through enhanced cGMP signalling in cerebellar Purkinje cells. *J. Physiol.* **591**, 1707–1730.
- Kitagawa, Y., Hirano, T., and Kawaguchi, S.Y. (2009). Prediction and validation of a mechanism to control the threshold for inhibitory synaptic plasticity. *Mol. Syst. Biol.* **5**, 280.
- Kohda, K., Kakegawa, W., Matsuda, S., Yamamoto, T., Hirano, H., and Yuzaki, M. (2013). The $\delta 2$ glutamate receptor gates long-term depression by coordinating interactions between two AMPA receptor phosphorylation sites. *Proc. Natl. Acad. Sci. USA* **110**, E948–E957.
- Konnerth, A., Dreessen, J., and Augustine, G.J. (1992). Brief dendritic calcium signals initiate long-lasting synaptic depression in cerebellar Purkinje cells. *Proc. Natl. Acad. Sci. USA* **89**, 7051–7055.
- Kubota, Y., and Bower, J.M. (2001). Transient versus asymptotic dynamics of CaM kinase II: possible roles of phosphatase. *J. Comput. Neurosci.* **11**, 263–279.
- Launey, T., Endo, S., Sakai, R., Harano, J., and Ito, M. (2004). Protein phosphatase 2A inhibition induces cerebellar long-term depression and declustering of synaptic AMPA receptor. *Proc. Natl. Acad. Sci. USA* **101**, 676–681.
- Lev-Ram, V., Nebyelul, Z., Ellisman, M.H., Huang, P.L., and Tsien, R.Y. (1997). Absence of cerebellar long-term depression in mice lacking neuronal nitric oxide synthase. *Learn. Mem.* **4**, 169–177.
- Lev-Ram, V., Wong, S.T., Storm, D.R., and Tsien, R.Y. (2002). A new form of cerebellar long-term potentiation is postsynaptic and depends on nitric oxide but not cAMP. *Proc. Natl. Acad. Sci. USA* **99**, 8389–8393.
- Lev-Ram, V., Mehta, S.B., Kleinfeld, D., and Tsien, R.Y. (2003). Reversing cerebellar long-term depression. *Proc. Natl. Acad. Sci. USA* **100**, 15989–15993.
- Lin, L.L., Wartmann, M., Lin, A.Y., Knopf, J.L., Seth, A., and Davis, R.J. (1993). cPLA2 is phosphorylated and activated by MAP kinase. *Cell* **72**, 269–278.
- Linden, D.J. (1996). A protein synthesis-dependent late phase of cerebellar long-term depression. *Neuron* **17**, 483–490.
- Linden, D.J. (2012). A late phase of LTD in cultured cerebellar Purkinje cells requires persistent dynamin-mediated endocytosis. *J. Neurophysiol.* **107**, 448–454.
- Linden, D.J., and Connor, J.A. (1991). Participation of postsynaptic PKC in cerebellar long-term depression in culture. *Science* **254**, 1656–1659.
- Lipina, C., and Hundal, H.S. (2017). The endocannabinoid system: ‘NO’ longer anonymous in the control of nitroergic signalling? *J. Mol. Cell Biol.* **9**, 91–103.
- Lüthi, A., Chittajallu, R., Duprat, F., Palmer, M.J., Benke, T.A., Kidd, F.L., Henley, J.M., Isaac, J.T.R., and Collingridge, G.L. (1999). Hippocampal LTD expression involves a pool of AMPARs regulated by the NSF-GluR2 interaction. *Neuron* **24**, 389–399.
- Malinow, R., and Malenka, R.C. (2002). AMPA receptor trafficking and synaptic plasticity. *Annu. Rev. Neurosci.* **25**, 103–126.
- Matsuda, S., Launey, T., Mikawa, S., and Hirai, H. (2000). Disruption of AMPA receptor GluR2 clusters following long-term depression induction in cerebellar Purkinje neurons. *EMBO J.* **19**, 2765–2774.
- Nabavi, S., Fox, R., Proulx, C.D., Lin, J.Y., Tsien, R.Y., and Malinow, R. (2014). Engineering a memory with LTD and LTP. *Nature* **511**, 348–352.
- Namiki, S., Kakizawa, S., Hirose, K., and Iino, M. (2005). NO signalling decodes frequency of neuronal activity and generates synapse-specific plasticity in mouse cerebellum. *J. Physiol.* **566**, 849–863.
- Newton, M., Niewczas, I., Clark, J., and Bellamy, T.C. (2010). A real-time fluorescent assay of the purified nitric oxide receptor, guanylyl cyclase. *Anal. Biochem.* **402**, 129–136.

- Noel, J., Ralph, G.S., Pickard, L., Williams, J., Molnar, E., Uney, J.B., Collingridge, G.L., and Henley, J.M. (1999). Surface expression of AMPA receptors in hippocampal neurons is regulated by an NSF-dependent mechanism. *Neuron* 23, 365–376.
- O’Flaherty, J.T., Chadwell, B.A., Kearns, M.W., Sergeant, S., and Daniel, L.W. (2001). Protein kinases C translocation responses to low concentrations of arachidonic acid. *J. Biol. Chem.* 276, 24743–24750.
- Piochon, C., Tittley, H.K., Simmons, D.H., Grasselli, G., Elgersma, Y., and Hansel, C. (2016). Calcium threshold shift enables frequency-independent control of plasticity by an instructive signal. *Proc. Natl. Acad. Sci. USA* 113, 13221–13226.
- Powell, K., Mathy, A., Duguid, I., and Häusser, M. (2015). Synaptic representation of locomotion in single cerebellar granule cells. *eLife* 4, 18.
- Safo, P.K., and Regehr, W.G. (2005). Endocannabinoids control the induction of cerebellar LTD. *Neuron* 48, 647–659.
- Sánchez, M.G., Ruiz-Llorente, L., Sánchez, A.M., and Díaz-Laviada, I. (2003). Activation of phosphoinositide 3-kinase/PKB pathway by CB(1) and CB(2) cannabinoid receptors expressed in prostate PC-3 cells. Involvement in Raf-1 stimulation and NGF induction. *Cell. Signal.* 15, 851–859.
- Sheng, M., and Lee, S.H. (2001). AMPA receptor trafficking and the control of synaptic transmission. *Cell* 105, 825–828.
- Shinomura, T., Asaoka, Y., Oka, M., Yoshida, K., and Nishizuka, Y. (1991). Synergistic action of diacylglycerol and unsaturated fatty acid for protein kinase C activation: its possible implications. *Proc. Natl. Acad. Sci. USA* 88, 5149–5153.
- Sossa, K.G., Beattie, J.B., and Carroll, R.C. (2007). AMPAR exocytosis through NO modulation of PICK1. *Neuropharmacology* 53, 92–100.
- Stamler, J.S., Simon, D.I., Osborne, J.A., Mullins, M.E., Jaraki, O., Michel, T., Singel, D.J., and Loscalzo, J. (1992). S-nitrosylation of proteins with nitric oxide: synthesis and characterization of biologically active compounds. *Proc. Natl. Acad. Sci. USA* 89, 444–448.
- Stephens, L.R., Eguinoa, A., Erdjument-Bromage, H., Lui, M., Cooke, F., Cadwell, J., Smrcka, A.S., Thelen, M., Cadwallader, K., Tempst, P., and Hawkins, P.T. (1997). The G beta gamma sensitivity of a PI3K is dependent upon a tightly associated adaptor, p101. *Cell* 89, 105–114.
- Su, L.D., Wang, D.J., Yang, D., Shen, Y., and Hu, Y.H. (2013). Retrograde cPLA2 α /arachidonic acid/2-AG signaling is essential for cerebellar depolarization-induced suppression of excitation and long-term potentiation. *Cerebellum* 12, 297–299.
- Tanaka, K., and Augustine, G.J. (2008). A positive feedback signal transduction loop determines timing of cerebellar long-term depression. *Neuron* 59, 608–620.
- Tanaka, K., Khiroug, L., Santamaria, F., Doi, T., Ogasawara, H., Ellis-Davies, G.C.R., Kawato, M., and Augustine, G.J. (2007). Ca²⁺ requirements for cerebellar long-term synaptic depression: role for a postsynaptic leaky integrator. *Neuron* 54, 787–800.
- Tsuruno, S., and Hirano, T. (2007). Persistent activation of protein kinase Calpha is not necessary for expression of cerebellar long-term depression. *Mol. Cell. Neurosci.* 35, 38–48.
- Tucker, D.E., Ghosh, M., Ghomashchi, F., Loper, R., Suram, S., John, B.S., Girotti, M., Bollinger, J.G., Gelb, M.H., and Leslie, C.C. (2009). Role of phosphorylation and basic residues in the catalytic domain of cytosolic phospholipase A2alpha in regulating interfacial kinetics and binding and cellular function. *J. Biol. Chem.* 284, 9596–9611.
- van Woerden, G.M., Hoebeek, F.E., Gao, Z., Nagaraja, R.Y., Hoogenraad, C.C., Kushner, S.A., Hansel, C., De Zeeuw, C.I., and Elgersma, Y. (2009). betaCaMKII controls the direction of plasticity at parallel fiber-Purkinje cell synapses. *Nat. Neurosci.* 12, 823–825.
- Vanhaesebroeck, B., and Waterfield, M.D. (1999). Signaling by distinct classes of phosphoinositide 3-kinases. *Exp. Cell Res.* 253, 239–254.
- Wang, Y.T., and Linden, D.J. (2000). Expression of cerebellar long-term depression requires postsynaptic clathrin-mediated endocytosis. *Neuron* 25, 635–647.
- Wang, D.J., Su, L.D., Wang, Y.N., Yang, D., Sun, C.L., Zhou, L., Wang, X.X., and Shen, Y. (2014). Long-term potentiation at cerebellar parallel fiber-Purkinje cell synapses requires presynaptic and postsynaptic signaling cascades. *J. Neurosci.* 34, 2355–2364.
- Yamaguchi, K., Itohara, S., and Ito, M. (2016). Reassessment of long-term depression in cerebellar Purkinje cells in mice carrying mutated GluA2 C terminus. *Proc. Natl. Acad. Sci. USA* 113, 10192–10197.